

Investigation of the phase composition in sintered lanthana-doped $(\text{Zr},\text{Sn})\text{TiO}_4$ ceramics

FLORIN VASILIU, SIMONA MOISA

Research Institute for Aircraft Materials, P.O. Box-24, R-76900, Bucharest-Magurele, Romania

DANIEL GROZEA

Institute of Physics and Technology of Materials, P.O. Box MG-7, R-76900, Bucharest-Magurele, Romania

CARMEN BUNESCU

METAV S.A., P.O. Box 18/3, R-71529, Bucharest, Romania

Ceramic materials of the $\text{ZrO}_2\text{-SnO}_2\text{-TiO}_2$ system, modified by La_2O_3 and ZnO additions, were investigated by X-ray diffraction, scanning electron microscopy and energy-dispersive X-ray spectrometry. All the samples sintered at 1330, 1360 and 1400 °C contain a $(\text{Zr}_x\text{Sn}_z)\text{TiO}_4$ ($x+z=1$, $0 < z \leq 0.4$) solid solution coexisting with ZrTiO_4 , the last gradually disappearing with rising temperature. At 1400 °C, the $(\text{Zr}_{0.8}\text{Sn}_{0.2})\text{TiO}_4$ solid solution matrix was not quite homogeneous, containing small amounts of a grain-boundary phase assumed to be $\text{La}_2(\text{Zr},\text{Sn},\text{Ti})_2\text{O}_7$ and the expected TiO_2 -basis solid solution rich in Zn and La . The evolution of the chemical composition of $(\text{Zr}_x\text{Sn}_z)\text{TiO}_4$ solid solution to $(\text{Zr}_{0.8}\text{Sn}_{0.2})\text{TiO}_4$ and the simultaneous disappearance of ZrTiO_4 are thought to explain the variation trends of lattice parameters with increasing sintering temperature.

1. Introduction

Materials from the system $(\text{Zr},\text{Sn})\text{TiO}_4$ are used as dielectric resonators, elements in microwave integrated circuits and microwave filters, due to their high dielectric constant and Q value, and their low temperature coefficient of resonant frequency [1–3]. These materials are generally difficult to sinter without additives, especially at lower temperatures. The sinterability increases with additions such as ZnO , NiO , MgO , CaO , Fe_2O_3 , and La_2O_3 [2, 4–6], used separately or in combination, but no mechanisms have been proposed for the improved densification kinetics or for the addition effect on the dielectric properties. The addition of Fe_2O_3 increased the dielectric loss due to a high-resistive spinel structure grain-boundary phase, whereas the NiO addition was effective in improving the Q value [2]. The La_2O_3 addition has been reported as an improving factor in sintering these ceramics, but the system $\text{ZrO}_2\text{-SnO}_2\text{-TiO}_2$ has been investigated only at the ends of the sintering temperature range, 1250–1350 °C [4], and at 1450 °C [5] in an oxygen atmosphere. A recent sol-gel method with metal alkoxides allowed the preparation of dense sintered compacts of $(\text{Zr}_x\text{Sn}_z)\text{TiO}_4$ ($x+z=1$), without any additives, at 1600 °C [3].

Solid solution formation in the system $\text{ZrO}_2\text{-SnO}_2\text{-TiO}_2$ was systematically investigated by X-ray diffraction, by Wolfram & Göbel [4] at 1250 °C $< T < 1350$ °C, and by McHale & Roth [7] at 1500 °C for 24 h and a subsequent thermal treat-

ment at 900 °C for 100 h. For an initial composition of 35:15:50 (mol %), the latter authors have found a solid solution of $(\text{Zr},\text{Sn},\text{Ti})_2\text{O}_4$ coexisting with another $(\text{Ti},\text{Sn})\text{O}_2$ solid solution persisting as detectable minor phase after heat treatment at 1485 °C. Wakino *et al.* [2] have reported a $(\text{Zr}_{0.8}\text{Sn}_{0.2})\text{TiO}_4$ material prepared with addition of Fe_2O_3 and 0.5% NiO , obtained at 1360 °C for 4 h, but although the composition of the solid solution within grains seemed to be homogeneous, at the grain boundaries spinel structure titanates such as $(\text{Zr},\text{Ni})_2\text{TiO}_4$ and $(\text{Zr},\text{Ni})\text{Fe}_2\text{O}_4$ were detected. However, quantitative X-ray microanalysis data of presumed single-phase $(\text{Zr}_{0.8}\text{Sn}_{0.2})\text{TiO}_4$ grains were not given.

In this paper, we present new structural investigation data for $(\text{Zr},\text{Sn})\text{TiO}_4$ prepared by classical ceramic technology, using reasonable sintering times and temperatures as reported by other authors [4–6]. Obviously, these specimens cannot be compared from the homogeneity degree point of view with those prepared by the same conventional solid-state reaction method, but using very long heat treatment and higher temperatures [7] or with those obtained by sintering monosized particles synthesized through the sol-gel method with metal alkoxides [3]. However, the investigated specimens of $(\text{Zr},\text{Sn})\text{TiO}_4$, doped with La_2O_3 and ZnO and sintered at 1400 °C, have stable dielectric characteristics and are reliable enough for use as microwave resonators. X-ray diffraction (XRD), scanning electron microscopy (SEM) and energy-dis-

persive X-ray spectrometry (EDX) were used to investigate the microstructure and phase composition of samples from $(\text{Zr},\text{Sn})\text{TiO}_4$ system.

2. Experimental procedure

Samples were prepared from reagent-grade ZrO_2 , SnO_2 , and TiO_2 , weighed to the desired amounts (according to the formula $(\text{Zr}_{0.8}\text{Sn}_{0.2})\text{TiO}_4$) equivalent to a molar composition ratio of 47:15:38. In order to obtain dense ceramics [2, 4–6], 1.5 wt % ZnO was added to all samples. The mixture was ball-milled in a planetary mill in distilled water for 2 h, dried, and calcined at 1050 °C for 2 h. After remilling with organic binder for 5 h, the powders were pressed into discs under 100 MPa. These discs were then placed on a Pt sheet in a fused Al_2O_3 crucible and sintered at 1330–1400 °C in air for 4 h. Reagent-grade La_2O_3 (0.5 wt %) was added to the starting materials, from the beginning, to a batch of samples.

XRD patterns of powders resulting from grinding and crushing of ceramic pellets were recorded by a diffractometer URD-6 (Zeiss), using CoK_α radiation. Secondary electron images and X-ray image maps were made using a scanning electron microscope SEM 515 (Phillips), equipped with EDX system, operating at a 16 KV acceleration voltage. The sintered ZST specimens were represented as

- A, 1330 °C sintering temperature
- B, 1330 °C sintering temperature, 0.5 wt % La_2O_3 addition
- C, 1360 °C sintering temperature
- D, 1360 °C sintering temperature, 0.5 wt % La_2O_3 addition
- E, 1400 °C sintering temperature
- F, 1400 °C sintering temperature, 0.5 wt % La_2O_3 addition

3. Experimental results and discussion

3.1. X-Ray diffraction data

The investigated samples were generally multiphase, except for those sintered at 1400 °C with La_2O_3 addition, which seemed to be biphasic and contained, besides the major orthorhombic phase $(\text{Zr}_{0.8}\text{Sn}_{0.2})\text{TiO}_4$, a TiO_2 solid solution with a small amount of Sn.

The specimens sintered at 1330 and 1360 °C (with or without La_2O_3 addition) and those sintered at 1400 °C without La_2O_3 addition, contained (besides the mentioned TiO_2 solid solution) two well-known isostructural orthorhombic phases ZrTiO_4 (ZT) and $(\text{Zr}_x\text{Sn}_z)\text{TiO}_4$, $x + z = 1$, $0 < z \leq 0.4$ (ZST) [4, 7]. The lattice parameters of the two orthorhombic compounds were determined using the peaks (022), (202), and (220) which showed either splittings or even isolated doublets. In order to assure a separation of overlapped doublets and an accurate determination of the lattice parameters, the X-ray peaks were recorded by step scanning with $0.01^\circ/2\theta$ step for 150 s measuring time. The data obtained were averaged and smoothed out by a computer.

The phase $(\text{Zr}_x\text{Sn}_z)\text{TiO}_4$ appeared as a solid solution with the composition depending on the sintering temperature. Thus the unit cell parameters of the samples sintered at 1330 and 1360 °C were close to those of the phase $(\text{Zr}_{0.6}\text{Sn}_{0.4})\text{TiO}_4$ ($z = 0.4$) and, respectively, the phase $(\text{Zr}_{0.7}\text{Sn}_{0.3})\text{TiO}_4$ ($z = 0.3$), both phases being known members of solid-solution series formed in the system ZrO_2 – SnO_2 – TiO_2 [4].

ZrTiO_4 was the major phase in samples sintered at 1330 °C, but its occurrence decreased at 1360 °C (in samples with or without La_2O_3) or at 1400 °C (without La_2O_3), and it disappeared completely in samples sintered at 1400 °C, with La_2O_3 addition. In samples C, D, and E, the major phase was the ZST solid solution with $0.2 < z \leq 0.4$.

Fig. 1 showed the variation of the lattice parameters of ZT phase and of ZST solid solution as a function of sintering temperature. Although the ZST lattice parameters belong to different components of the solid solution series with various chemical compositions, the graph of their dependence on sintering temperature is however shown, just to point out a comparison with the analogous variation for ZT phase.

The unit cell parameters were on the whole in agreement with those reported by other authors [4, 7–9], but there were some noteworthy differences. The values obtained for the a_0 parameter were generally lower and for c_0 greater than those known for

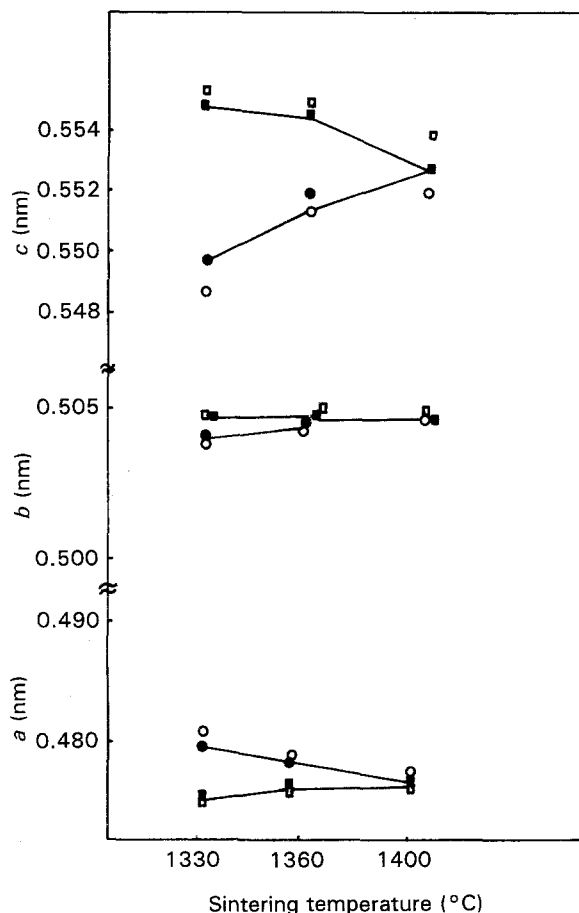


Figure 1 Experimentally observed variation of lattice parameters with sintering temperature for ZST and ZT phases. \circ , ZT; \square , ZST specimens without La_2O_3 ; \bullet , ZT; \blacksquare , ZST specimens with La_2O_3 addition.

pure ZT quenched from 1500 °C after a thermal treatment for 44 h [7] or those of samples sintered from oxide powders at 1600 °C [3]. However, the trends of a slight rise in a_0 , constant b_0 , and a marked increase in c_0 with sintering temperature were similar to the variation of the lattice parameters as a function of quenching temperature, previously reported.

For the ZST solid solution found in our sintered samples, the inverse variation of a_0 and c_0 lattice parameters as compared to that for a ZST solid solution with a fixed composition [3, 7] could be explained by the compositional changes induced by sintering temperature increase and oxide addition.

During sintering, the phases ZT and ZST had opposed variation trends of the a_0 and c_0 lattice constants, as shown in Fig. 1, which suggested a correlation between the phase separation and dissolution processes. The corresponding unit cell parameters of the two phases exhibited closer and closer values with increasing sintering temperature. For both phases, the constancy of b_0 observed previously for all the members of ZST solid solution and for pure ZT [3, 4, 7, 9], was also verified in this case. The ZT a_0 and c_0

parameters showed a variation of maximum 0.7% and those of ZST solid solution of 0.4%. These values were similar to the relative characteristic variation for pure sintered ZT, registered for a larger temperature range 1000–1400 °C [3], and were in good agreement with the relative variation of c_0 ($<0.5\%$) found on the conversion of the high-temperature form to the low-temperature structure of pure ZT [7]. On the other hand, according to previous structural data [3, 7] regarding ZST, the variation of the lattice parameters a_0 and c_0 was in the range 0.3–0.5%, for a quenching temperature from 1000 to 1400 °C.

3.2. SEM and EDX results

Secondary electron images showed a rather porous structure of all samples, some of them with a distinctly revealed polyhedral grain morphology. For instance, Fig. 2 shows characteristic microstructural aspects of specimens A, B, E, and F.

In La_2O_3 -doped, sintered specimens, an increased average grain size and a reduction of porosity were

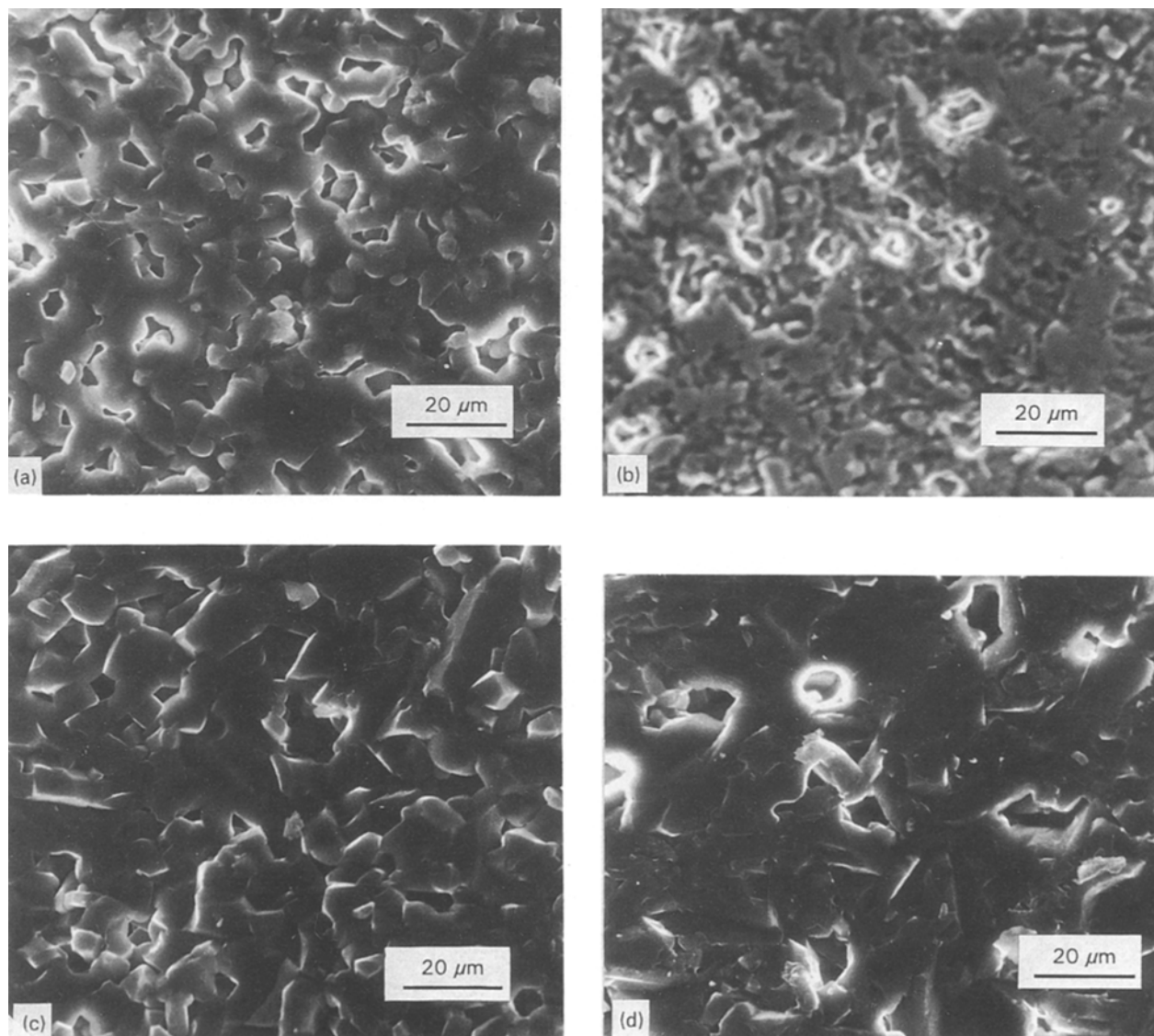


Figure 2 Microstructures of as-sintered surfaces of ZST specimens: (a) 1330 °C, ZnO; (b) 1330 °C, $\text{La}_2\text{O}_3 + \text{ZnO}$; (c) 1400 °C, ZnO; (d) 1400 °C, $\text{La}_2\text{O}_3 + \text{ZnO}$.

found at the same sintering temperature. La_2O_3 addition appeared more efficient in promoting the densification of samples sintered at 1330°C , where a drastic decrease in pore concentration was registered, whereas the pore density values were only weakly modified at 1400°C . For samples without La_2O_3 , the sintering temperature rise from 1330 to 1400°C led to a slight increase in the average and maximum grain size, and to a marked reduction in pore concentration. A preponderantly linear pore morphology and an interconnected porosity at 1330°C and a closed one at 1400°C were found.

Density measurements through the Archimedes method in deionized water confirmed the observed sintering behaviour. The specimen density was found to increase in the following sequence: $\text{A} \rightarrow \text{C} \rightarrow \text{B} \rightarrow \text{D} \rightarrow \text{E} \rightarrow \text{F}$. Therefore the optimal sintering was achieved for La_2O_3 -doped specimens sintered at 1400°C . Quantitative EDX data confirmed the coexistence of both ZT and ZST phases in specimens A, B, C, D, and E. A solid solution of ZST with $z = 0.4$ was registered in specimens A and B, and another with $z = 0.3$ was identified in specimens C, D, and E.

In Fig. 3, SEM pictures and X-ray image maps of elements Sn, Zn and La for an area of sample surface F are presented. The back-scattered image (Fig. 3a) reveals clearly, besides the pore distribution, the presence of two distinct phases in the matrix: a dark phase, consisting of polyhedral and acicular particles with dimensions of $2\text{--}7\ \mu\text{m}$, and a finer white phase having $1\text{--}3\ \mu\text{m}$ particle dimensions. Distributions of Ti and Sn (Fig. 3b) are relatively homogeneous, unlike the distributions of Zn (Fig. 3c) or La (Fig. 3d). The two latter figures show a greater concentration of elements Zn and La in the area of the dark phase and the white phase, respectively.

A quantitative EDX analysis of the same F specimen is given in Table I for zones marked in Fig. 3a: 1 (matrix), 2 (dark phase), and 3 (white phase). The matrix phase was found to have a formula $\text{Zr}_{0.74}\text{Sn}_{0.26}\text{TiO}_4$, close to the $(\text{Zr}_{0.8}\text{Sn}_{0.2})\text{TiO}_4$ solid solution detected by XRD. The dark phase, Ti-rich and with appreciable amounts of Zn and La, could be identified with a TiO_2 -basis solid solution incorporating dopant atoms and a very small quantity of Sn.

At the point marked 3 (Fig. 3a), an intergranularly precipitated secondary phase (not detectable by XRD)

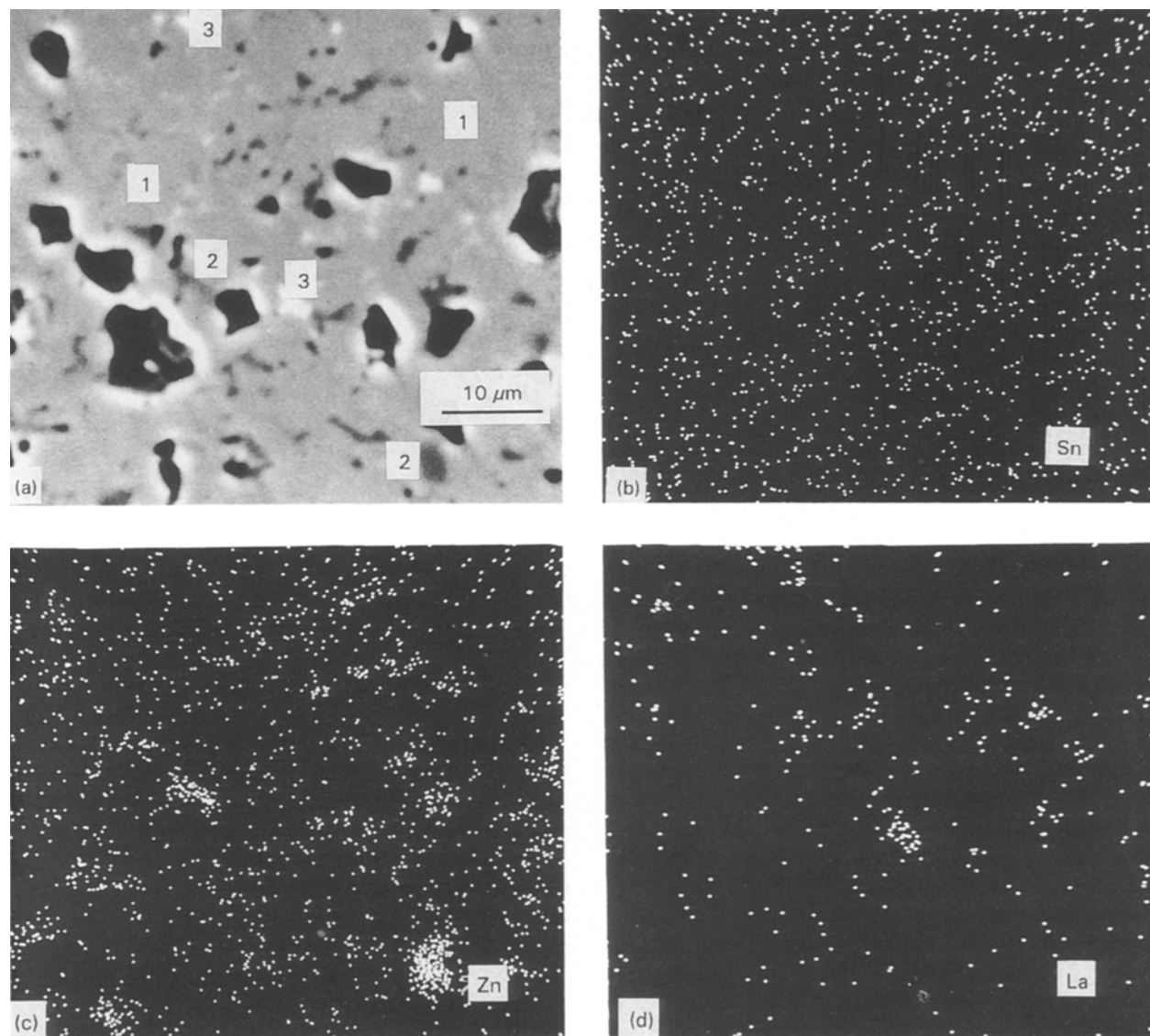


Figure 3 Back-scattered electron image (a), and X-ray image maps: Sn (b); Zn (c); and La (d) for a polished surface specimen sintered at 1400°C with 1.5 wt% ZnO and 0.5 wt% La_2O_3 .

TABLE I True concentration values for component elements (at %)

Point	Zr	Ti	Sn	Zn	La
1	33.28	54.34	11.75	0.63	–
2	3.80	65.61	3.37	16.54	10.68
3	37.45	28.00	6.58	–	27.97

was identified as being compatible with a formula $(\text{Zr}_{0.75}\text{La}_{0.5}\text{Sn}_{0.15})\text{Ti}_{0.6}\text{O}_4$ or equivalent $(\text{Zr},\text{La},\text{Sn})_{1.4}\text{Ti}_{0.6}\text{O}_4$, but no information is available concerning the possibility of the Zr substitution by La, although some lanthanide oxides (such as CeO_2) can form solid solutions with ZrO_2 . Perhaps, by analogy with the $\text{La}_2\text{Ti}_2\text{O}_7$ compound, a chemical formula for the secondary phase given by $\text{La}_2(\text{Zr},\text{Sn},\text{Ti})_2\text{O}_7$ is more plausible. This secondary phase, occurring especially at grain boundaries, was relatively close (except for the amount of La) to $\text{ZrSn}_{0.5}\text{Ti}_{0.5}\text{O}_4$, which was a phase equivalent to $(\text{Zr},\text{Sn})_{1.5}\text{Ti}_{0.5}\text{O}_4$, already reported by Wolfram & Göbel [4]. Therefore the matrix solid solution was not completely homogeneous even after sintering at 1400°C , in spite of the evidence of the XRD data.

The results presented were in part different from those previously reported by Wolfram & Göbel [4] and McHale & Roth [7] because the $(\text{Zr}_{0.8}\text{Sn}_{0.2})\text{TiO}_4$ solid solution was reached only in samples sintered at 1400°C with La_2O_3 addition, even if the same initial molar composition ratio of 47:15:38 was used for all the samples. McHale & Roth [7] reported, for a molar composition ratio of 35:15:50, the formation of two solid solutions $(\text{Zr},\text{Sn},\text{Ti})_2\text{O}_4$ and $(\text{Ti},\text{Sn})\text{O}_2$, but Hirano *et al.* [3] obtained similar results only for as-precipitated powders with Sn content of $z > 0.3$, and a single-phase $(\text{Zr}_x\text{Sn}_z)\text{TiO}_4$ solid solution at values of $z < 0.3$. Filhol *et al.* [10] showed the formation of a biphasic composition, but specified only one of the phases as being $(\text{Zr}_{0.6}\text{Sn}_{0.4})\text{TiO}_4$ in samples sintered at $1320\text{--}1380^\circ\text{C}$ for 0.5 or 8 h.

A possible explanation of the above-mentioned structural differences could be connected with the following factors: (i) the increased addition of ZnO ; (ii) the formation of an intergranular phase rich in dopants, similar to those previously detected for other addition elements [2], which could influence the volume and grain diffusion of Sn; and (iii) the effect of some phase nucleation processes, not yet investigated, connected with the homogeneity degree and calcination behaviour of the initial oxide powders. The influence of powder preparation methods on the dielectric properties of the $(\text{Zr},\text{Sn})\text{TiO}_4$ system was already reported [5, 10] and their role in the formation of the single-phase solid solution in this case could be analogous to that played in the preparation of the single phase compound $\text{Ba}_2\text{Ti}_9\text{O}_{20}$ [11].

The phase coexistence in the $\text{ZrO}_2\text{--SnO}_2\text{--TiO}_2$ system can be explained by microscopic compositional fluctuations resulting from the preparation technique, which cannot provide a truly atomic homogeneity in the solid solution. The compositional fluctuations can lead to the formation of very small

regions richer in Sn (ZST solid solution with $z < 0.2$) as a function of microscopic concentration and temperature gradients. The increase of sintering temperature enhanced the diffusion effects within and between these regions and led to a relative homogenization of the local composition, more quickly reached in the La_2O_3 -doped specimens. Eventually, the occurrence of a single-phase $(\text{Zr}_{0.8}\text{Sn}_{0.2})\text{TiO}_4$ solid solution as the major phase of the system was observed.

4. Conclusions

1. An optimal sintering for ZnO and La_2O_3 -doped $\text{ZrO}_2\text{--SnO}_2\text{--TiO}_2$ materials (molar starting composition 47:15:38) was found at 1400°C .
2. All the samples sintered at 1330, 1360 and 1400°C (in the last case, without La_2O_3 addition) contained a ZST solid solution, coexisting with a TiO_2 -basis solid solution and with ZrTiO_4 . ZT occurrence decreased with the temperature raising, until a complete disappearance in La_2O_3 -doped samples, sintered at 1400°C .
3. According to the XRD data, the $(\text{Zr}_{0.8}\text{Sn}_{0.2})\text{TiO}_4$ solid solution, formed as a major phase in La_2O_3 -doped specimens sintered at 1400°C , appeared as homogeneous, but EDX measurements also revealed a secondary phase with a composition given by $(\text{Zr},\text{La},\text{Sn})_{1.4}\text{Ti}_{0.6}\text{O}_4$, probably close to the $\text{La}_2(\text{Zr},\text{Sn},\text{Ti})_2\text{O}_7$ phase. Remanent TiO_2 -basis solid solution was found rich in Zn and La.
4. Variation trends of lattice parameters with sintering temperature for ZT phase and ZST solid solution showed a correlation between the evolution of the chemical composition of ZST solid solution towards the formula $(\text{Zr}_{0.8}\text{Sn}_{0.2})\text{TiO}_4$ and the gradual disappearance of ZrTiO_4 . A possible explanation for this behaviour was eventually given, but it was evident that the occurrence of a homogeneous single-phase $(\text{Zr}_{0.8}\text{Sn}_{0.2})\text{TiO}_4$ solid solution was strongly dependent on the sintering process parameters.

References

1. K. WAKINO, *Ferroelectrics* **91** (1989) 69.
2. K. WAKINO, K. MINAI and H. TAMURA, *J. Amer. Ceram. Soc.* **67** (1984) 278.
3. S. HIRANO, T. HAYASHI and A. HATTORI, *ibid.* **74** (1991) 1320.
4. G. WOLFRAM and H. E. GÖBEL, *Mater. Res. Bull.* **16** (1981) 1455.
5. J. C. MAGE and C. DELJURIE, Brevet d'Invention No. 80 04601, Paris, France, 1980.
6. A. E. McHALE, R. KUDESIA and A. H. LEE, in Proceedings of a Symposium on Electroceramics, Solid State Ionics, edited by H. L. Tuller and D. M. Smyth (1988) p. 88.
7. A. E. McHALE and R. S. ROTH, *J. Amer. Ceram. Soc.* **66** (1983) C18.
8. A. E. McHALE and R. S. ROTH, *ibid.* **69** (1986) 827.
9. R. E. NEWNHAM, *ibid.* **50** (1967) 216.
10. P. FILHOL, G. GAQUERE, G. DESGARDIN, P. LAFPEZ and C. DELJURIE, in Proceedings of a Conference on Dielectric Resonators for Satellite Broadcasting, Lannion, France, 1980, p. A7/1–8.
11. J. M. WU and H. W. WANG, *J. Amer. Ceram. Soc.* **71** (1988) 869.

Received 19 February
and accepted 10 December 1993